Combination brain and systemic injections of AAV provide maximal functional and survival benefits in the Niemann-Pick mouse

Marco A. Passini*†, Jie Bu*, Jonathan A. Fidler*, Robin J. Ziegler*, Joseph W. Foley*, James C. Dodge*, Wendy W. Yang*, Jennifer Clarke*, Tatyana V. Taksir*, Denise A. Griffiths*, Michael A. Zhao*, Catherine R. O'Riordan*, Edward H. Schuchman‡, Lamya S. Shihabuddin*, and Seng H. Cheng*

*Genzyme Corporation, Framingham, MA 01701; and ‡Mount Sinai School of Medicine, New York, NY 10029

Communicated by Richard L. Sidman, Harvard Institutes of Medicine, Boston, MA, April 16, 2007 (received for review February 26, 2007)

Niemann-Pick disease (NPD) is caused by the loss of acid sphingomyelinase (ASM) activity, which results in widespread accumulation of undegraded lipids in cells of the viscera and CNS. In this study, we tested the effect of combination brain and systemic injections of recombinant adeno-associated viral vectors encoding human ASM (hASM) in a mouse model of NPD. Animals treated by combination therapy exhibited high levels of hASM in the viscera and brain, which resulted in near-complete correction of storage throughout the body. This global reversal of pathology translated to normal weight gain and superior recovery of motor and cognitive functions compared to animals treated by either brain or systemic injection alone. Furthermore, animals in the combination group did not generate antibodies to hASM, demonstrating the first application of systemic-mediated tolerization to improve the efficacy of brain injections. All of the animals treated by combination therapy survived in good health to an investigator-selected 54 weeks, whereas the median lifespans of the systemic-alone, brain-alone, or untreated ASM knockout groups were 47, 48, and 34 weeks, respectively. These data demonstrate that combination therapy is a promising therapeutic modality for treating NPD and suggest a potential strategy for treating disease indications that cause both visceral and CNS pathologies.

acid sphingomyelinase | adeno-associated virus | immunotolerization | lysosomal storage disease | neurodegeneraton

The majority of lysosomal storage diseases (LSDs) contain both CNS and visceral pathologies. Current experimental designs in animal models use either intracranial injection of viral vectors to treat the neurodegenerative disease (1–15) or systemic delivery of these vectors to treat the visceral organs (15–24). However, the exclusive use of either delivery route may not be optimal in the clinic because both compartments may need correction to achieve a meaningful quality of life and an increased lifespan. Designing an experimental paradigm that incorporates multiple delivery strategies may provide increased benefit for disease indications with whole-body pathology.

Niemann-Pick disease (NPD) is an example of an LSD that exhibits pathologies in both the viscera and CNS. NPD is caused by a genetic deficiency of acid sphingomyelinase (ASM), with resultant accumulation of sphingomyelin (SPM) and cholesterol in many visceral tissues such as the liver, lung, and spleen, as well as the brain and spinal cord (24). The accumulation of these substrates in the lysosomes leads to dysregulation of normal cellular function and presentation of a variety of altered phenotypes, including hepatosplenomegly and pulmonary failure, which are predominant in Type B patients, and progressive neurodegeneration, mental retardation, and early death in Type A patients.

An ASM knockout (ASMKO) mouse model of NPD recapitulates the visceral and brain pathologies of the human disease (25, 26). Previous studies of ASMKO mice showed that intracranial injections of adeno-associated virus (AAV) serotype vectors encoding human ASM (hASM) decreased the burden of storage in the brain (10, 12). Furthermore, tail vein injections of AAV8-hASM, with resultant hepatic transduction and secretion of hASM, effectively reduced lysosomal pathology in the viscera and cellular inflammation in the lung (19). However, these studies did not demonstrate long-term functional recovery and survival. In the present report, we tested the effects of combination brain and systemic injections of AAV on lifespan, storage pathology, and motor and cognitive functions in the ASMKO mouse. Our data demonstrated that combination injections were superior to either brain- or systemic-only injection in all aspects of substrate correction, functional recovery, and survival. Importantly, it affirmed the benefits of multiple gene-delivery strategies in disease indications with whole-body pathology.

Results

Expression of hASM in ASMKO Mice After Single or Combination Brain and Systemic Injections of AAV-hASM Vectors. We examined whether a combination injection protocol of AAV-hASM that targets both body compartments would be efficacious in addressing the functional abnormalities and disease sequelae of the ASMKO mouse. In the combination group ($n = 11$), ASMKO mice at 4 weeks of age received 3.0×10^{11} genome copies (gc) of AAV8-hASM via tail vein injection. Two weeks later, at 6 weeks of age, the same mice were injected with AAV2-hASM into four sites in the right and left sides of the brain. Each site was injected with 1.5×10^{10} gc, for a total of 1.2×10^{11} gc per brain. AAV2 was chosen for brain–gene transfer because this AAV serotype is currently the only one in use in clinical trials for neurodegeneration. The treated control groups received only systemic injections of AAV8-hASM at 4 weeks of age ($n = 12$) or only brain injections of AAV2-hASM at 6 weeks of age ($n = 14$), and the untreated control groups included ASMKO ($n = 23$) and wild-type ($n = 10$) mice.

Analysis of the serum from ASMKO mice treated by systemic injection alone and by combination injections exhibited the highest levels of circulating hASM (Fig. 1*A*). Transduction and subsequent expression by AAV8-hASM was likely hepatic-mediated because of the tropism of this viral serotype and the selection of a liver-restricted promoter (DC190) in the design of the expression cassette (18, 19, 27). Both groups attained peak levels of hASM at 2

Author contributions: M.A.P. designed research; M.A.P., J.B., J.A.F., R.J.Z., J.W.F., J.C.D., W.W.Y., J.C., T.V.T., D.A.G., M.A.Z., and C.R.O. performed research; M.A.P., E.H.S., L.S.S., and S.H.C. analyzed data; and M.A.P. and S.H.C. wrote the paper.

The authors declare no conflict of interest.

Freely available online through the PNAS open access option.

Abbreviations: AAV, adeno-associated virus; ASM, acid sphingomyelinase; ASMKO, ASM knockout; BMT, bone marrow transplantation; gc, genome copies; hASM, human ASM; LSD, lysosomal storage disease; NPD, Niemann-Pick disease; SPM, sphingomyelin.

†To whom correspondence should be addressed. E-mail: marco.passini@genzyme.com.

This article contains supporting information online at www.pnas.org/cgi/content/full/0703509104/DC1.

NEUROSCIENCE

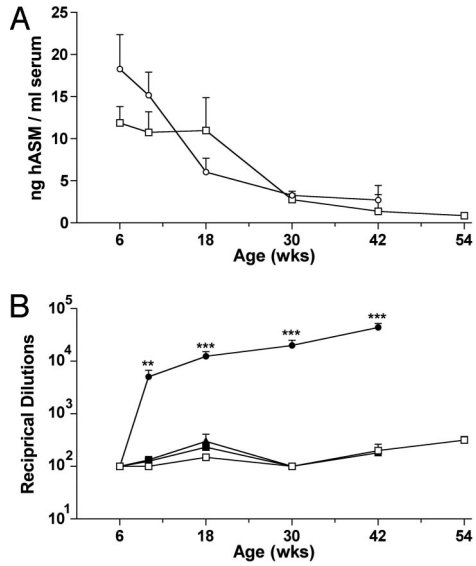

Fig. 1. Levels of hASM and anti-hASM antibodies in the viscera. ELISAs were performed on serum from periodic eye bleeds to determine the levels of hASM (*A*) and anti-hASM (*B*) antibodies in circulation. Shown are the significant *P* values that compare the individual groups to untreated ASMKO mice. *, $P < 0.05$; **, $P < 0.01$; ***, $P < 0.001$. Filled square, untreated ASMKO mice; open square, combination group; open circle, AAV8 systemic-alone group; filled circle, AAV2 brain-alone group.

weeks postinjection, followed by a moderate decrease in protein levels over the 1-year period of the study, which may be because of the cellular turnover that naturally occurs in the liver. hASM was also detected in the liver, lung, spleen, and muscle of mice treated by combination or AAV8 systemic-alone injections [supporting information (SI) Fig. 7]. There were no detectable levels of hASM in the serum and visceral tissue from the AAV2 brain-alone and untreated ASMKO groups. Blood serum also showed that the levels of anti-hASM antibody in mice treated by combination or AAV8 systemic-alone injections were similar to the low, baseline levels observed in untreated ASMKO mice (Fig. 1*B*). In contrast, mice from the AAV2 brain-alone group exhibited a rapid and robust induction of anti-hASM antibody titers (Fig. 1*B*). Hence, animals treated by systemic injection of AAV8-hASM were immunotolerized to the expressed hASM.

All biochemical and histological assays were performed at endpoints determined on humane grounds or arbitrarily set at an investigator-selected 54 weeks. Analysis of the brain from the combination and AAV2 brain-alone groups showed high levels of hASM throughout the neuraxis (Fig. 2*A*). However, the combination group exhibited significantly higher levels of hASM despite the use of the same recombinant AAV2 vector in both groups. The levels of hASM in brains of mice treated solely by systemic injection were comparable to those in untreated ASMKO mice, which indicated that circulating hASM was not able to traverse the blood–brain barrier into the CNS. Interestingly, the titer of anti-hASM antibody in brain homogenates was significantly higher in the AAV2 brain-alone group compared to the other groups, including the combination group (Fig. 2*B*). Thus, the enzyme levels in the brain were reciprocal of the antibody titers; the combination group showed high levels of hASM and low levels of anti-hASM antibodies, whereas the AAV2 brain-alone group showed low levels of hASM and high levels of anti-hASM antibodies. There was no evidence of cellular infiltration and no increase in microglia activation in the AAV2 brain-alone group (SI Fig. 8), suggesting that the immunological response in this group was restricted to the humoral system.

Effect of hASM Expression at Correcting Storage Pathology in the Viscera and Brain of ASMKO Mice. There was complete correction of SPM storage in all visceral tissues examined from the AAV8 systemic-alone and combination groups (Fig. 3*A*). In contrast, animals that received only brain injections were similar to untreated ASMKO mice in containing high visceral levels of SPM. Analysis of SPM in the brains of the combination group showed global reduction of the substrate to wild-type levels (Fig. 3*B*). This correction was a substantial improvement over the AAV2 brain-alone group, which exhibited a significant decrease of SPM only in those brain slabs corresponding to an injection site (Fig. 3*B*). Thus, at the dose tested, the extent of correction in the brain-alone group was significantly less and never approached the efficacy observed in the combination group. The

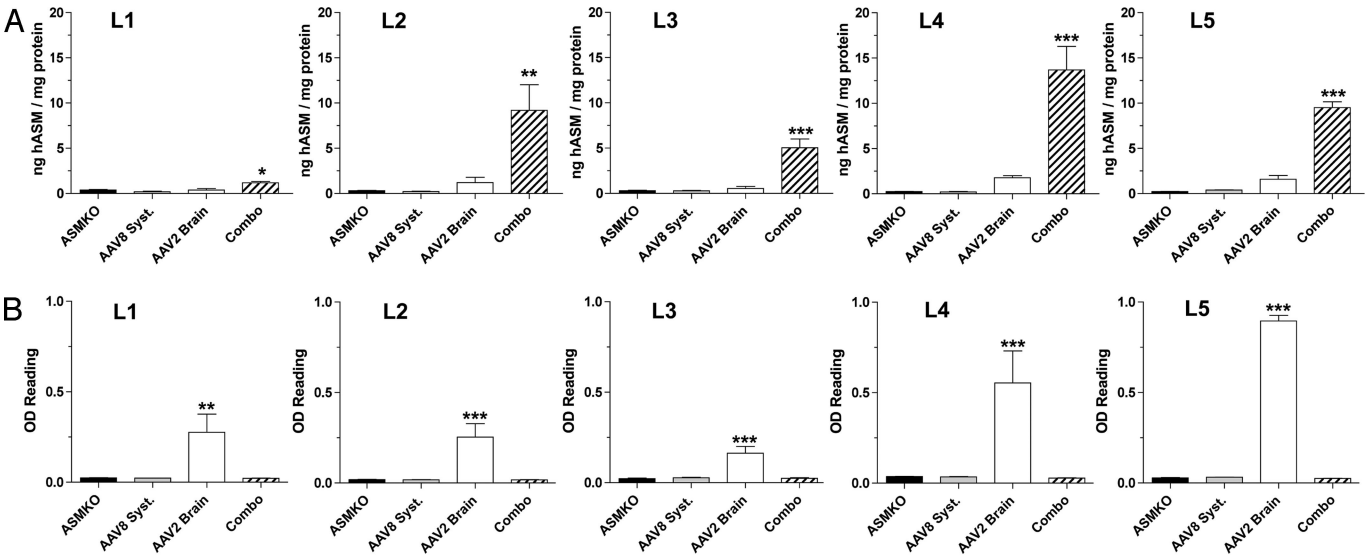

Fig. 2. Levels of hASM and anti-hASM antibodies in brain homogenates. The combination group contained significantly higher levels of hASM compared to the AAV2 brain-alone group throughout the entire brain (*A*). The same homogenates were used to measure anti-hASM antibody levels in the brain (*B*). See Fig. 3*B* for the relative positions of L1–L5 along the neuraxis. *, $P < 0.05$; **, $P < 0.01$; ***, $P < 0.001$. ASMKO, untreated ASMKO mice; combo, combination group; AAV8 syst, AAV8 systemic-alone group; AAV2 brain, AAV2 brain-alone group; WT, untreated wild-type mice.

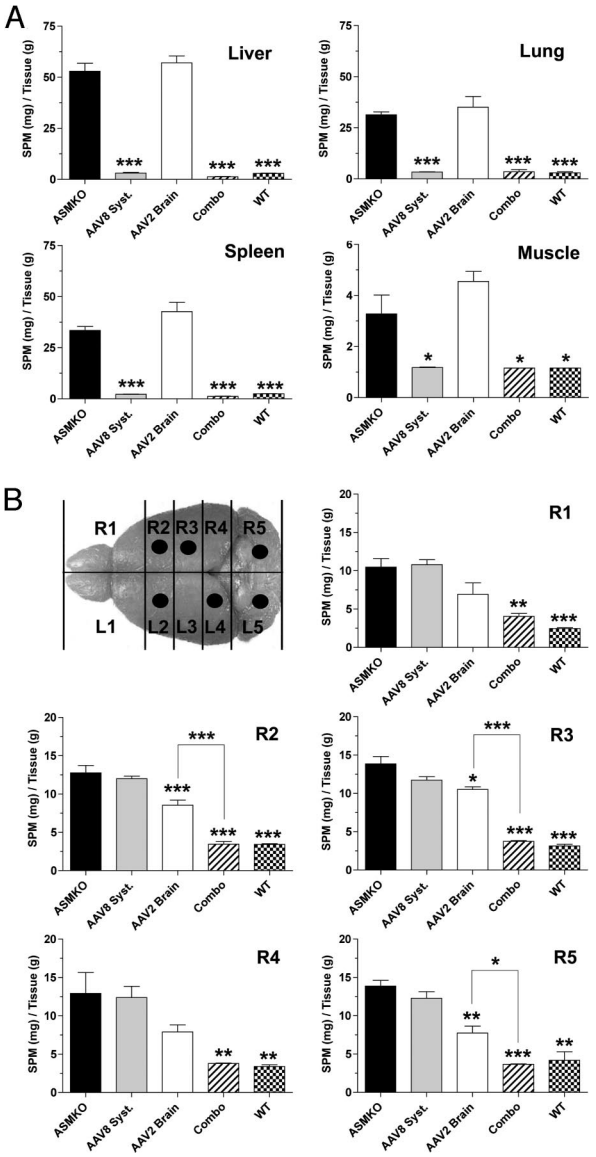

Fig. 3. Sphingomyelin levels in the viscera and brain. Shown are levels of SPM storage in the liver, lung, spleen, and skeletal muscle (*A*), and in the brain (*B*). The illustration shows the relative positions of the five brain slabs along the neuraxis, and the dots correspond to the brain slabs that contained an injection site. *, $P < 0.05$; **, $P < 0.01$; ***, $P < 0.001$. ASMKO, untreated ASMKO mice; combo, combination group; AAV8 syst, AAV8 systemic-alone group; AAV2 brain, AAV2 brain-alone group; WT, untreated wild-type mice.

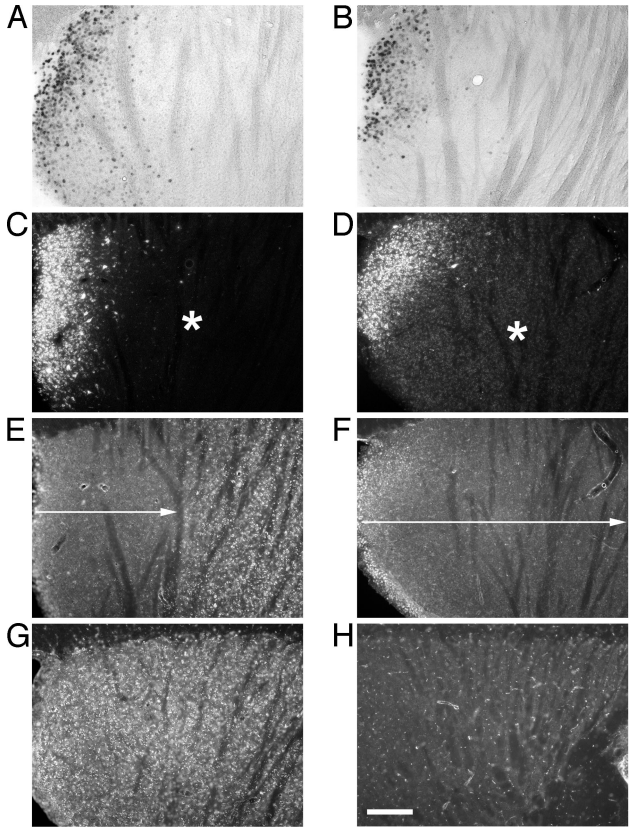

Fig. 4. Correlation of hASM expression and reversal of pathology in the brain. Shown are sagittal tissue sections of the striatum from the AAV2 brain-alone (*A*, *C*, and *E*), combination (*B*, *D*, and *F*), and untreated ASMKO (*G*) and wild-type (*H*) groups. Brain sections were processed by *in situ* hybridization to determine the site of transduction (*A* and *B*), by immunohistochemistry to detect hASM (*C* and *D*), and by lysenin to detect SPM (*E–H*). The hASM human mRNA and protein patterns in the AAV2 brain-alone group roughly overlapped with the area of SPM clearance (arrow). In contrast, animals from the combination group showed clearance of SPM (arrow) that extended beyond the transduction site. On closer examination, a faint and diffuse hASM pattern that may correspond to cross-correction was observed in the combination group (asterisk). This diffuse hASM pattern was not observed in the AAV2 brain-alone group (asterisk), indicating that cross-correction may have been compromised in this group. All photographs were exposure-matched for accurate comparisons. (Scale bar: 0.25 mm.)

less-efficient reduction of SPM storage in the AAV2 brain-alone group correlated with the lower levels of enzyme observed in this group. High levels of brain SPM, similar to the levels in untreated ASMKO mice, were found in the AAV8 systemic-alone group.

The pattern of hASM expression and the clearance of SPM storage overlapped in the AAV2 brain-alone group (Fig. 4). In contrast, the correction of SPM storage extended beyond the transduction site in animals that received combination therapy. Similar patterns were observed with the cholesterol marker, filipin (SI Fig. 9). Large regions of the brain were cleared of cholesterol storage in the combination group, whereas only local and more limited clearance of cholesterol was observed in the AAV2 brain-alone group. Hence, the ability of hASM to diffuse from the sites of transduction to correct storage pathology in distal regions of the brain was significantly better in mice treated by combination injections compared to mice that received only brain injection. The AAV8 systemic-alone group did not show any measurable correction of SPM (data not shown) or cholesterol (SI Fig. 9) storage in the brain.

Effect of AAV-hASM on Motor Function, Cognition, and Survival. Animals in the combination group showed significant improvements of motor performance on both the accelerating (Fig. 5*A*) and rocking (Fig. 5*B*) rotarod tests at all time points examined ($P < 0.001$). Mice treated by only AAV2 brain injections showed a modest improvement in motor performance on the accelerating rotarod at early time points when compared to the untreated ASMKO mice. However, their performance deteriorated at later time points, demonstrating that brain-alone injections were not sufficient to sustain the correction in motor function. With the rocking rotarod, which is a more stringent test of motor function and coordination, the AAV2 brain-alone group performed poorly throughout the entire study. The AAV8 systemic-alone group showed little to no benefit on either rotarod test.

Mice were tested for cognitive function on the Barnes maze,

NEUROSCIENCE

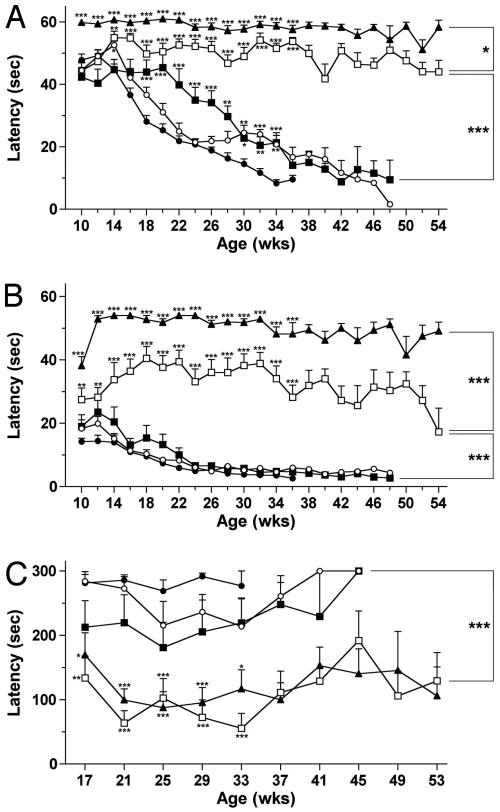

Fig. 5. Restoration of motor and cognitive function in ASMKO mice. Analysis of motor function by accelerating (*A*) and rocking (*B*) rotarods, and cognitive function by the Barnes maze (*C*). The combination group performed significantly better than untreated ASMKO and AAV2 brain- and AAV8 systemic-alone groups on both rotarod tests throughout the entire time course ($P <$ 0.001). However, the combination group was not completely asymptomatic when compared to untreated wild-type controls (*A* and *B*). In the Barnes maze, the combination group performed at wild-type levels throughout the time course of the study, which did not occur in the singly treated groups (*C*). *, $P <$ 0.05; **, $P < 0.01$; ***, $P < 0.001$. In addition, comparisons between the AAV2 brain-alone group and the combination group, and between the combination group and untreated wild-type mice, are shown in brackets. Open square, combination group; open circle, AAV8 systemic-alone group; filled square, AAV2 brain-alone group; filled circle, untreated ASMKO mice; filled triangle, untreated wild type.

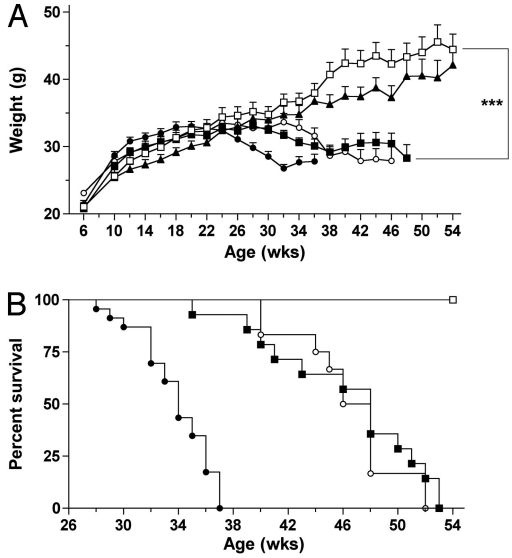

Fig. 6. Comparison of fitness and survival benefits. Animals in the combination group gained weight over time, similar to wild-type controls (*A*). In contrast, the AAV2 brain- and AAV8 systemic-alone groups lost weight during the late stages of survival. The Kaplan–Meier curve shows that all mice in the AAV2 brain- and AAV8 systemic-alone groups became moribund (*B*). In contrast, 100% of the ASMKO mice receiving combination therapy survived to 54 weeks of age. *, $P < 0.05$; **, $P < 0.01$; ***, $P < 0.001$. In addition, comparison between the AAV2 brain-alone group and the combination group is shown in brackets. Open square, combination group; open circle, AAV8 systemic-alone group; filled square, AAV2 brain-alone group; filled circle, untreated ASMKO mice; filled triangle, untreated wild type.

which requires the use of memory-mediated spatial navigation cues to escape the adverse light stimulus (28). The AAV2 brain-alone group performed better than untreated ASMKO, but never approached the performance level observed in wild-type mice (Fig. 5*C*). Mice treated by systemic injections alone showed marginal improvement when compared to untreated controls. In contrast, on the Barnes maze, the combination group performed with a proficiency similar to wild-type mice ($P > 0.05$).

Mice were weighed biweekly to evaluate overall fitness (Fig. 6*A*), and their survival was plotted on a Kaplan–Meier curve (Fig. 6*B*). The combination group had a weight-gain profile similar to wild-type animals, which was significantly better than the AAV2 brain- and AAV8 systemic-alone groups ($P < 0.001$). Moribund animals (defined as heavy ataxia, inability to walk in a straight line without tumbling over, inability to groom, loss of 20% body weight, and dehydration) were killed on humane grounds. The combination, AAV2 brain-, and AAV8 systemic-alone groups displayed increased survival compared to untreated ASMKO mice, which had a median lifespan of 34 weeks. However, all of the ASMKO mice treated by combination therapy survived in good health to 54 weeks of age (Fig. 6*B*). This survival benefit was a significant improvement over the AAV2 brain- and AAV8 systemic-alone groups, in which all animals eventually became moribund with median lifespans of 48 and 47 weeks, respectively ($P < 0.0001$). None of the animals in the singly treated groups survived to 54 weeks. Thus, treating the CNS or viscera separately did not fully protect ASMKO mice from premature death.

Discussion

Previous studies of LSD animal models showed that intracranial or tail vein injections of viral vectors were effective in treating the disease only in the respective compartments (15). Therefore, combination therapy may provide increased therapeutic efficacy for LSDs with whole-body pathology. The ASMKO mouse was a suitable animal model to test this experimental modality because it exhibits whole-body pathology that recapitulates the human disease.

The combination protocol used in this study was highly efficacious and mediated increased benefits compared to animals receiving systemic- or brain-only injection. The targeting of both the viscera and brain resulted in global reversal of storage pathology, which translated to preservation of motor and cognitive functions at near-normal levels. Furthermore, ASMKO mice treated by combination therapy showed normal weight gain, no recognizable ataxia, and greater longevity. Of particular importance was the ability of combination therapy to provide significant functional improvement to at least 54 weeks, the oldest age examined. This observation indicates that combination therapy provides mice with an improved quality of life during the period of extended survival. This efficacy was a significant improvement over the singly treated groups, which showed an ≈40% increase in lifespan compared to untreated ASMKO mice, but poor performances on functional tests. Thus, although targeting the brain or viscera separately for correction could moderately extend the longevity of ASMKO mice,

these mice experienced a relatively poorer quality of life that included heavy ataxia, poor gait, and malnutrition. Although animals in the combination group showed a remarkable improvement in rotarod performance, future studies that evaluate the spinal cord and peripheral nervous system may help elucidate why these animals were not completely asymptomatic compared to untreated wild-type controls.

Animals in the combination group contained lower levels of anti-hASM antibodies in both blood and brain homogenates compared to the AAV2 brain-alone group, which indicated that immunotolerization to the expressed hASM occurred in the combination group. This observation is consistent with previous studies in which minimal antibodies against hASM, human α-galactosidase, and glucocerebrosidase were generated in animals treated by systemic injections of AAV8 vectors when the transgene was placed under the transcriptional control of a liver-specific promoter (18, 19, 23, 24, 29). However, the data in the current study are the first examples of applying systemic-mediated tolerization to improve the efficacy of brain injections. This synergism provided the combination group with widespread levels of therapeutic hASM and global reduction of lipid storage in the brain that were significantly better than levels in animals receiving only brain injections.

Differential patterns of hASM distribution and reversal of pathology occurred in the brain. Animals from the combination group showed clearance of SPM and cholesterol storage that extended beyond the sites of transduction, whereas animals that received only brain injections contained more localized areas of lipid correction that closely overlapped with the sites of transduction. These data suggest that cross-correction was limited in the AAV2 brain-alone group presumably because of the presence of anti-hASM antibodies. A mechanism by which antibodies bind to the secreted enzyme and prevent their endocytosis from the extracellular space would explain the lack of global reversal of pathology in the AAV2 brain-alone group. In contrast, immunotolerization in the combination group prevented an antibody response against hASM, which resulted in efficient secretion, exposure, and uptake of therapeutic enzymes in large regions of the brain.

Generation of antibodies against lysosomal enzymes constitutes an important limitation in cell and gene therapy protocols. In another ASMKO study, systemic injections of bone marrow cells into ablated newborn mice, in combination with mesenchymal stem cell injections into the brain, resulted in Purkinje cell survival and a modest preservation of motor function in the ASMKO mouse (30). However, there was an eventual decline in behavioral function that correlated with a rise in anti-hASM antibodies (30). Furthermore, an immunological response to α-L-iduronidase after cell- or gene-based therapies to the brain of mucopolysaccharidosis type 1 dogs resulted in significant inflammation and poor therapeutic efficacy (31, 32). These reports underscore the benefits accruing from prevention of antibody formation against the therapeutic protein and the utility of the AAV8-DC190 vector system used in this study to achieve immunotolerance for more efficient, sustained expression of the transgene product and functional recovery.

Combination brain and systemic injections of therapeutic agents have been performed in other LSD mouse models. Enzyme replacement therapy to treat the visceral disease, in combination with bone marrow transplantation (BMT) to address the brain disease, was efficacious in the mucopolysaccharidosis type VII mouse (33). Substrate deprivation therapy, together with BMT in the Sandhoff mouse, also provided reversed pathology and improved survival (34). However, similar to the earlier NPD study (30), radiation-mediated ablation of the recipients' marrow was required for efficient engraftment of transplanted cells (33, 34). Furthermore, therapeutic efficacy in the mucopolysaccharidosis type I dog was achieved only when immunosuppression was performed before brain injections of an AAV vector (32). Coinjection of both recombinant AAV and BMT in the Twitcher mouse brain resulted in improved survival only when performed in the presence of myeloreductive radiation (35). In contrast, the dual viral vector injection system for combination therapy developed in the current study may not require preconditioning of the host or the chronic use of immunosuppression, which would be advantageous in the clinic. Demonstration of immunotolerization in large animal models, including primates, will be needed before this strategy is translated to humans.

In conclusion, we showed that combination brain and systemic injections of AAV vectors encoding hASM are a promising therapeutic modality for treating NPD. Targeting both the brain and viscera translated to improved functional recovery and prolonged survival compared to animals treated by only one route of delivery. Furthermore, the establishment of immunotolerance before brain injection highlighted the benefits of addressing the immune response to the transgene product for achieving increased correction of the CNS manifestations. The information in this study may provide a clinical strategy for diseases presenting with whole-body pathology and for neurological disorders that may be adversely affected by antibodies generated against the therapeutic protein.

Materials and Methods

Recombinant AAV Vectors. AAV8-hASM contained serotype-2 inverted terminal repeats and the hASM cDNA under the control of the DC190 liver-restricted promoter (18, 19, 23). AAV2-hASM contained serotype-2 inverted terminal repeats and the hASM cDNA under the control of the CMV enhancer-chicken β-actin promoter. Both recombinant vectors were produced by triple-plasmid cotransfection of human 293 cells and were column-purified as reported (36). The final titers of AAV8-hASM and AAV2-hASM were 5.0×10^{12} gc/ml as determined by *Taq*Man PCR of the bovine growth hormone polyadenylation signal sequence.

Animal Surgery. All animal handling and surgeries were performed under a protocol approved by the Institutional Animal Care and Use Committee. The genotypes of ASMKO mice were confirmed by PCR (26). ASMKO mice at 4 weeks received AAV8-hASM tail vein injections and were separated into two groups. One group, designated as "AAV8 systemic-alone," underwent no further surgery. The other group, designated as "combination," were injected into the brain 2 weeks later by stereotaxic surgery. A third group of ASMKO mice, designated as "AAV2 brain-alone," were injected into the brain at 6 weeks without prior systemic treatment. All ASMKO mice that underwent brain surgery were injected into the hypothalamus (−0.50 mm, −1.00 mm, −3.50 mm), hippocampus (−2.00, −1.75, −1.75), medulla (−6.00, −1.50, −3.75), and cerebellum (−6.00, −1.50, −2.25) on the right side of the brain, and into the striatum (0.50, 1.75, −2.75), motor cortex (0.50, 1.75, −1.25), midbrain (−4.50, 1.00, −3.50), and cerebellum (−6.00, 1.50, −2.25) on the left side of the brain. Injections were performed with a Hamilton syringe (Hamilton, Reno, NV) at a rate of 0.5 μl/min.

Animal Perfusion. Animals were killed according to a humane protocol approved by the Institutional Animal Care and Use Committee. All untreated ASMKO mice and ASMKO mice in the AAV2 brain- and AAV8 systemic-alone groups eventually became moribund. In contrast, ASMKO mice treated by combination therapy remained in good health, but were nonetheless killed at 54 weeks for comparative analysis. Thus, all of the animals killed in this study ranged in age from 28 to 54 weeks (see Fig. 6*B*). Animals from each group were perfused through the heart with PBS to remove all blood and equally divided into biochemical and histological cohorts. In the biochemical cohort, the liver, lung, spleen, skeletal muscle, and brain were removed. The brain was bisected sagitally, and each side was cut trans-

versely into five 2- to 3-mm slabs along the A–P axis. Slabs from the left hemisphere were analyzed for hASM protein and anti-hASM antibodies, and those from the right hemisphere were analyzed for SPM storage. In the histological cohort, animals were perfused with 4% paraformaldehyde, and tissues were sectioned on a vibratome as reported (37).

Measurement of hASM and Anti-hASM Antibody Levels. An ELISA with rabbit polyclonal antibodies specific for hASM (Genzyme) was used to quantify the level of protein in tissue and serum samples as reported (19). The serum levels of anti-hASM antibodies were determined by an ELISA (19). Titers were defined as the reciprocal of the highest dilution of serum that produced an $OD_{450} \geq 0.1$. With the expectation that antibodies within the brain parenchyma would be at lower concentrations than in serum, the assay method was modified by diluting tissue lysates 1:20 in antibody dilution buffer and applying samples in duplicate to a 96-well plate coated with 100 ng hASM. The secondary antibody HRP conjugate and chromogenic substrate reactions were carried out as reported (19). The concentration of anti-hASM antibody correlated directly with the color intensity of the HRP reaction from the conjugate, and the final data were reported as the absolute change in OD_{450}.

Assay for Sphingomyelin Levels. Quantification of SPM levels in tissue samples was performed as reported (10, 19). SPM in tissue extracts was quantified with the Amplex Red sphingomyelinase kit (Molecular Probes, Eugene, OR), with purified SPM C18 (Matreya, Pleasant Gap, PA) as standards. Sphingomyelin levels were normalized per gram wet weight of tissue.

Histological Assays. Brain sections were analyzed for hASM protein with an anti-hASM biotinylated monoclonal antibody (Genzyme) at a dilution of 1:200 and visualized as reported (12). For microglia activation, an F4/80 antibody (Genzyme) at 1:10 dilution was incubated overnight and visualized with a biotinylated goat anti-rat secondary antibody (Vector Laboratories, Burlingame, CA). *In situ* hybridization was performed to determine the hASM mRNA pattern (12). Cholesterol was detected in brain sections with a filipin-staining protocol (12). Lysenin staining was done to determine the SPM substrate distribution pattern (37).

Behavioral Testing. Beginning at 10 weeks of age, mice were tested biweekly on the accelerating and rocking rotarods by using the Smartrod Program (AccuScan Instruments, Columbus, OH). The speed of the cylinder rotation on the accelerating rotarod was programmed to accelerate at a constant rate from 0 to 30 rpm over 60 sec, and the rocking rotarod was programmed to accelerate forward and backward every 2.5 sec to a final speed of 25 rpm over 54 sec. Four trials were performed with each animal at each time point, and the latency to fall from the platform was recorded.

Beginning at 17 weeks of age, mice were tested every 4 weeks on the Barnes maze (San Diego Instruments, San Diego, CA), a flat, circular apparatus for measuring learning and memory in rodents. An aversive, nonnociceptive stimulus in the form of four 300-W overhead lights was placed 160 cm above the surface of the maze (28). The maze contained 20 equally spaced holes along the periphery. Only one hole contained an escape chamber that allowed a mouse to evade the aversive light stimulus by using visual cues located on the surface of the maze and walls. Mice were tested once per day for 4 consecutive days (38). The first 3 days were training, and data on day 4 were collected for statistical analysis. The cut-off time was 300 sec.

Statistics. The amounts of hASM protein, anti-hASM antibody, SPM levels, and the latencies on the rotarods and Barnes maze were analyzed with one-way ANOVA and Dunnet's posttest. The Kaplan–Meier survival curve was analyzed with the log-rank test equivalent to the Mantel–Haenszel test. All statistical analyses were performed with GraphPad Prism version 4.0 (GraphPad Software, San Diego, CA). All values with $P < 0.05$ or better were considered significant.

We thank Antonius Song, Denise Woodcock, and Shelley Nass (Genzyme Corporation) for AAV vectors; and Leah Curtin, Karen Norton, and David Koske for animal maintenance.

1. Skorupa AF, Fisher KJ, Wilson JM, Parente MK, Wolfe JH (1999) *Exp Neurol* 160:17–27.
2. Bosch A, Perret E, Desmaris N, Heard JM (2000) *Mol Ther* 1:63–70.
3. Sferra TJ, Qu G, McNeely D, Rennard R, Clark KR, Lo WD, Johnson PR (2000) *Hum Gene Ther* 11:507–519.
4. Frisella WA, O'Connor LH, Vogler CA, Roberts M, Walkley S, Levy B, Daly TM, Sands MS (2001) *Mol Ther* 3:351–358.
5. Fu H, Samulski RJ, McCown TJ, Picornell YJ, Fletcher D, Muenzer J (2002) *Mol Ther* 5:42–49.
6. Passini MA, Lee EB, Heuer GG, Wolfe JH (2002) *J Neurosci* 22:6437–6446.
7. Cressant A, Desmaris N, Verot L, Brejot T, Froissart R, Vanier MT, Maire I, Heard JM (2004) *J Neurosci* 24:10229–10239.
8. Desmaris N, Verot L, Puech JP, Caillaud C, Vanier MT, Heard JM (2004) *Ann Neurol* 56:68–76.
9. Griffey M, Bible E, Vogler C, Levy B, Gupta P, Cooper J, Sands MS (2004) *Neurobiol Dis* 16:360–369.
10. Dodge JC, Clarke J, Song A, Bu J, Yang W, Taksir TV, Griffiths D, Zhao Q, Schuchman EH, Cheng SH, *et al.* (2005) *Proc Natl Acad Sci USA* 102:17822–17827.
11. Liu G, Martins I, Wemmie JA, Chiorini JA, Davidson BL (2005) *J Neurosci* 25:9321–9327.
12. Passini MA, Macauley SL, Huff MR, Taksir TV, Bu J, Wu I, Piepenhagen PA, Dodge JC, Shihabuddin LS, O'Riordan CR, *et al.* (2005) *Mol Ther* 11:754–762.
13. Vite CH, McGowan JC, Niogi SN, Passini MA, Drobatz KJ, Haskins ME, Wolfe JH (2005) *Ann Neurol* 57:355–364.
14. Passini MA, Dodge JC, Bu J, Yang W, Zhao Q, Sondhi D, Hackett NR, Kaminsky SM, Mao Q, Shihabuddin LS, *et al.* (2006) *J Neurosci* 26:1334–1342.
15. Sands MS, Davidson BL (2006) *Mol Ther* 13:839–849.
16. Watson GL, Sayles JN, Chen C, Elliger SS, Elliger CA, Raju NR, Kurtzman GJ, Podsakoff GM (1998) *Gene Ther* 5:1642–1649.
17. Jung SC, Han IP, Limaye A, Xu R, Gelderman MP, Zerfas P, Tirumalai K, Murray GJ, During MJ, Brady RO, *et al.* (2001) *Proc Natl Acad Sci USA* 98:2676–2681.
18. Ziegler RJ, Lonning SM, Armentano D, Li C, Souza DW, Cherry M, Ford C, Barbon CM, Desnick RJ, Gao G, *et al.* (2004) *Mol Ther* 9:231–240.
19. Barbon CM, Ziegler RJ, Li C, Armentano D, Cherry M, Desnick RJ, Schuchman EH, Cheng SH (2005) *Mol Ther* 12:431–440.
20. Sun B, Zhang H, Franco LM, Young SP, Schneider A, Bird A, Amalfitano A, Chen YT, Koeberl DD (2005) *Mol Ther* 11:57–65.
21. Koeberl DD, Sun BD, Damodaran TV, Brown T, Millington DS, Benjamin DK, Jr, Bird A, Schneider A, Hillman S, Jackson M, *et al.* (2006) *Gene Ther* 13:1281–1289.
22. Sun B, Zhang H, Benjamin DK, Jr, Brown T, Bird A, Young SP, McVie-Wylie A, Chen YT, Koeberl DD (2006) *Mol Ther* 14:822–830.
23. McEachern KA, Nietupski JB, Chuang WL, Armentano D, Johnson J, Hutto E, Grabowski GA, Cheng SH, Marshall J (2006) *J Gene Med* 8:719–729.
24. Ziegler RJ, Cherry M, Barbon CM, Li C, Bercury SD, Armentano D, Desnick RJ, Cheng SH (2006) *Mol Ther*, 10.1038/sj.mt.6300066.
25. Schuchman EH, Desnick RJ (2001) in *The Metabolic and Molecular Basis of Inherited Disease*, eds Scriver CR, Beaudet AL, Sly WS, Valle D (McGraw-Hill, New York), pp 3589–3610.
26. Horinouchi K, Erlich S, Perl DP, Ferlinz K, Bisgaier CL, Sandhoff K, Desnick RJ, Stewart CL, Schuchman EH (1995) *Nat Genet* 10:288–293.
27. Gao GP, Alvira MR, Wang L, Calcedo R, Johnston J, Wilson JM (2002) *Proc Natl Acad Sci USA* 99:11854–11859.
28. Barnes CA (1979) *J Comp Physiol Psychol* 93:74–104.
29. Franco LM, Sun B, Yang X, Bird A, Zhang H, Schneider A, Brown T, Young SP, Clay TM, Amalfitano A, *et al.* (2005) *Mol Ther* 12:876–884.
30. Jin HK, Schuchman EH (2003) *Mol Ther* 8:876–885.
31. Lutzko C, Kruth S, Abrams-Ogg AC, Lau K, Li L, Clark BR, Ruedy C, Nanji S, Foster R, Kohn D, *et al.* (1999) *Blood* 93:1895–1905.
32. Ciron C, Desmaris N, Colle MA, Raoul S, Joussemet B, Verot L, Ausseil J, Froissart R, Roux F, Cherel Y, *et al.* (2006) *Ann Neurol* 60:204–213.
33. Sands MS, Vogler C, Torrey A, Levy B, Gwynn B, Grubb J, Sly WS, Birkenmeier EH (1997) *J Clin Invest* 99:1596–1605.
34. Jeyakumar M, Norflus F, Tifft CJ, Cortina-Borja M, Butters TD, Proia RL, Perry VH, Dwek RA, Platt FM (2001) *Blood* 97:327–329.
35. Lin D, Donsante A, Macauley SM, Levy B, Vogler C, Sands MS (2007) *Mol Ther* 15:44–52.
36. O'Riordan CR, Lachapelle AL, Vincent KA, Wadsworth SC (2000) *J Gene Med* 2:444–454.
37. Shihabuddin LS, Numan S, Huff MR, Dodge JC, Clarke J, Macauley SL, Yang W, Taksir TV, Parsons G, Passini MA, *et al.* (2004) *J Neurosci* 24:10642–10651.
38. Fox GB, Fan L, LeVasseur RA, Faden AI (1998) *J Neurotrama* 15:1037–1046.